Discussions

Geoscientific
Instrumentation
Methods and
Data Systems

Optimization of CPMG sequences for NMR borehole measurements

M. Ronczka and M. Müller-Petke

Leibniz Institute for Applied Geophysics, Hannover, Germany

Correspondence to: M. Ronczka (mathias.ronczka@liag-hannover.de)

Optimization of CPMG sequences for NMR borehole

M. Ronczka and M. Müller-Petke

Full Screen / Esc

Printer-friendly Version

Interactive Discussion

Abstract

Nuklear Magnetic Resonance (NMR) can provide key information such as porosity and permeability for hydrological characterization of geological material. Especially the NMR transverse relaxation time T_2 is used to estimate permeability since it reflects a
⁵ pore-size dependent relaxation process. The measurement sequence (CPMG) usually used consists of several thousands of electromagnetic pulses to densely record the relaxation process. These pulses are equidistantly spaced by a time constant τ.

In NMR borehole applications the use of CPMG sequences for measuring the transverse relaxation time T_2 is limited due to requirements on energy consumption. It is
¹⁰ state of the art to conduct at least two sequences with different echo spacings (τ) for recording fast and slow relaxing processes that correspond to different pore-sizes. For the purpose to reduce the amount of energy used for conducting CPMG sequences and to obtain both, slow and fast, decaying components within one sequence we tested the usage of CPMG sequences with an increasing τ and a decreasing number of pulses.
¹⁵ A synthetic study as well as laboratory measurements on samples of glass beads and granulate of different grain size spectra were conducted to evaluate the effects of of an increasing τ spacing, e.g. an enhanced relaxation due to diffusion processes.

The results are showing broadened T_2 distributions if the number of pulses is decreasing and the mean grain size is increasing, which is mostly an effect of a signifi-
²⁰ cantly shortened acquisition time. The shift of T_2 distributions to small decay times in dependence of the τ spacing and the mean grain size distribution is observable.

We found that it is possible to conduct CPMG sequences with an increased τ spacing. According to the acquisition time and enhanced diffusion the sequence parameters (number of pulses and τ_{max}) has to be chosen carefully. Otherwise the underestimated
²⁵ relaxation time (T_2) will lead to misinterpretations.

Title Page

Abstract · Introduction

Conclusions · References

Tables · Figures

|◄ · ►|

◄ · ►

Back · Close

Full Screen / Esc

Printer-friendly Version

Interactive Discussion

1 Introduction

The method of Nuclear Magnetic Resonance (NMR), discovered in the forties of the last century (Bloch et al., 1946; Purcell et al., 1946), has found widespread use in scientific and daily life. It was not later than the sixties that a first borehole tool was developed (Brown and Gamson, 1960) to take advantages of the unique properties of NMR in geophysics. It allows a direct detection and quantification of water since the initial amplitude of an NMR signal corresponds to the amount of protons exited. Furthermore, the measured decay time depends on the pore geometry and can therefore be used to estimate hydraulic permeabilities (Seevers, 1966).

There has been significant changes in the design of borehole tools in the nineties (Miller et al., 1990) using artificial magnetic fields and measurement sequences (CPMG after Carr and Purcell, 1954; Meiboom and Gill, 1958) that made NMR a frequently used tool in oil and gas exploration.

Laboratory NMR commonly conducts CPMG sequences with several thousand pulses and a short equidistant pulse spacing (τ) to densely record the decaying signal and to ensure a sufficient acquisition time. Each of this pulses causes an NMR echo being the measured signal (Hahn, 1950). Thus, τ is referred to be the echo spacing of a CPMG sequence. Until now it is common to conduct at least two different CPMG sequences in NMR borehole measurements. While slow decaying components are acquired with a sequence consisting of 1000 pulses and a large echo spacing (τ), fast decaying components can be measured with only a few dozens of echos and a short echo spacing (Kruspe et al., 2009). In this paper we present an optimized CPMG sequence that records both, slow and fast decaying, parts of an NMR signal within one CPMG sequence.

Besides applications in oil and gas exploration, NMR borehole measurements are needed in near-surface groundwater investigation. There are several reasons NMR logging is unused for this purpose. Standard NMR logging of groundwater monitoring wells is far too expensive. Monitoring wells are of diameters as small as two inches,

i.e. a large diameter NMR tool cannot be used. Consequently, a commercially available small diameter NMR tool is needed that was introduced by Vista-Clara in 2011. However, this tool is using an external power supply and is not interoperable with the standard logging equipment used. It is this huge energy needed for CPMG pulse sequences that limits the construction of a small diameter tool, which is interoperable with logging equipment usually used in near-surface logging business. Therefore, researches for developing an NMR borehole tool to characterise groundwater layers are in progress. As part of this project an additional demand for modified CPMG sequence is needed to consume a minimum amount of energy. This can be reached by reducing the number of pulses recorded and adjusting the echo spacing (τ) between the pulses.

For the purpose to reduce the amount of energy used while conducting CPMG sequences and to obtain slow and fast decaying components, we tested the usage of CPMG sequences with an increasing echo spacing and decreasing number of echos. For testing CPMG sequences with different parameter sets and various ways of increasing τ a synthetic study was performed. In order to have sufficient control on pore-size, laboratory measurements were conducted on samples of glass beads and granulate of different grain size spectra. This helps to cover a broad range of material that may be observed in field experiments.

2 NMR – T_2 relaxation

2.1 Free induction decay

As a property of matter, namely the spin, a hydrogen proton posses a microscopic magnetic moment. In a static magnetic field B_0 a torque is applied that lead to an orientation of the magnetic moments along the stream lines of that field. According to the field strength of B_0 the protons precess with the Larmor frequency $\omega_L = \gamma \cdot B_0$ about the stream lines of B_0, where γ [Hz T^{-1}] is the gyromagnetic ratio. If an electromagnetic pulse (B_1) with the frequency ω_L perpendicular to B_0 is applied, the protons can

M. Ronczka and
M. Müller-Petke

be flipped about an angle dependent on the pulse duration and amplitude. Immediately after terminating the excitation pulse, all affected protons returning (relax) to the equilibrium state, i.e. the direction of the external static magnetic field (B_0). During relaxation the protons precessing about the stream lines of B_0. If the stream lines of B_0
5 denote the z-direction the relaxation process is observed in the x-y-plane. The decay in the x-y-plane can be described by Eq. (1).

$$M_{xy}(t) = M_0 \cdot e^{\left(\frac{-t}{T_2}\right)} \tag{1}$$

Here, M_0 is the initial amplitude, T_2 the transverse relaxation time and M_{xy} the magnetisation in the x-y-plane. For further information on basic NMR theory we refer to
10 Dunn et al. (2002) or Coates et al. (1999). Basic parameters of interest are the initial amplitude M_0 at $t = 0$, due to it's sensitivity on water content and the relaxation time T_2, as an indicator of pore space properties. Hence, the transverse relaxation time T_2 denotes how fast or slow the magnetisation decreases in the x-y-plane.

All effects that lead to T_2 relaxation are inhomogeneities in the magnetic field,
15 i.e. magnetic gradients. These can be large scaled, like variations in the field strength of B_0, or small scaled due to particles with a significant magnetic susceptibility in the porous medium. Various magnetic field intensities lead to slightly different Larmor frequencies and therefore to a loss of phase coherence in the x-y-plane. The precession of protons in the x-y-plane under the influence of internal magnetic gradients is illus-
20 trated schematically in Fig. 1. At $t = t_0$ all protons are coherent. Slightly different Larmor frequencies results in a dephasing of the protons, which causes a reduced transverse magnetization M_0.

The relaxation time T_2^* consists of three parts, the bulk relaxation $T_{2,\text{B}}$, the surface relaxation $T_{2,\text{S}}$ and the relaxation due to any kind of dephasing $T_{2,\text{P}}$. All parts are parallel
25 processes and can be expressed via Eq. (2) (Coates et al., 1999).

$$\frac{1}{T_2^*} = \frac{1}{T_{2,\text{B}}} + \frac{1}{T_{2,\text{S}}} + \frac{1}{T_{2,\text{P}}} \tag{2}$$

The bulk relaxation $T_{2,B}$ denotes the relaxation time of free water, the surface relaxation $T_{2,S}$ describes any influences of the pore surface to the protons in the vicinity of the surface and $T_{2,P}$ includes all kinds of magnetic gradients (macroscopic, microscopic).

2.2 T_2-relaxation

All influences of macroscopic magnetic gradients can be avoided by conducting a CPMG sequence (Carr and Purcell, 1954; Meiboom and Gill, 1958). In this case $T_{2,P}$ can be simplified to a diffusion term $T_{2,D}$, which is governed by internal or microscopic magnetic gradients. The diffusion relaxation $T_{2,D}$ occur due to proton movements trough these magnetic gradients. While moving, the relaxating protons pass through regions with varying magnetic field strengths, which results in a changing Larmor frequency. According to these differences in the Larmor frequency the protons loses their phase coherence. This diffusion effect is non-removable. The diffusion term can be expressed via Eq. (3), e.g. (Keating and Knight, 2007),

$$\frac{1}{T_{2,D}} = D\frac{(\gamma G \tau)^2}{12} \tag{3}$$

with the gradient G [G cm^{-1}] of the magnetic field, γ [Hz T^{-1}] the gyromagnetic ratio, D [m^2 s^{-1}] the diffusion coefficient and τ [s] the spacing between an echo and the inducing pulse. As $T_{2,P}$ can be reduced to $T_{2,D}$, Eq. (2) transforms to Eq. (4), which now describes all effects that influences the T_2 decay time.

$$\frac{1}{T_2} = \frac{1}{T_{2,B}} + \frac{1}{T_{2,S}} + D\frac{(\gamma G \tau)^2}{12}. \tag{4}$$

According to Eq. (3) diffusion effects can be minimized by choosing a small τ while conducting a CPMG sequence. If the diffusion term can be assumed to be negligible, only $T_{2,B}$ and $T_{2,S}$ affect the decay time in Eq. (4). Equation (3) also indicates that diffusion effects take more effect if the echo spacing τ is to large.

Optimization of CPMG sequences for NMR borehole

M. Ronczka and
M. Müller-Petke

2.3 Estimation of pore size by means of T_2

According to Eq. (4) the transverse relaxation time T_2 measured by a CPMG sequence consists of $T_{2,B}$ and $T_{2,S}$. The bulk relaxation $T_{2,B}$ denotes the relaxation of free water. Here the protons are only affected by other protons during relaxation. The surface relaxation $T_{2,S}$ includes all effects of the grain surface that lead to a faster relaxation. These effects imply magnetic properties and the structure of the inner surface of the material. The surface relaxation, assuming a fast diffusion regime (Brownstein and Tarr, 1979), can be expressed by Eq. (5).

$$\frac{1}{T_{2,S}} = \rho \frac{S}{V}$$
(5)

Whereas ρ [$\mathrm{m\,s^{-1}}$] denotes the surface relaxivity, S [$\mathrm{m^2}$] the surface and V [$\mathrm{m^3}$] the volume of a pore. According to Eq. (5) the influence of surface relaxation increases for small pores and/or large surface relaxivities. Due to these dependencies, fine material with small pores will create a faster decaying signal compared to coarse material. Thus, knowing the surface relaxivity (ρ) it is possible to calculate a pore radius. If, for example, a spherical pore geometry is assumed, the surface to volume ratio ($\frac{S}{V}$) equals $\frac{6}{d}$ or if a cylindrical geometry is assumed $\frac{S}{V} = \frac{1}{d}$ (without top and bottom).

3 CPMG sequences

3.1 Classic CPMG

The CPMG sequence consists of an excitation pulse (P90), which flips the orientation of the macroscopic magnetisation about 90° from the z-direction into the x-y-plane and several refocusing pulses (P180), which flips the protons about 180° in the x-y-plane. After the excitation pulse (P90) the protons losing their phase coherence due to slightly different Larmor frequencies, caused by magnetic gradients. After a time span τ

a refocusing pulse (P180) is applied, which flips the protons in a manner that those with a higher ω_L lag behind those with a lower one. Due to refocusing an echo is building up and reaches its maximum after $2 \times \tau$. The maximum of the echo marks the point of maximal coherence of the protons.

5   In general τ is constant over the whole CPMG sequence and has to be very small to ensure that the diffusion term is negligible, otherwise the protons are not refocused completely, which lead to a reduced amplitude of the echo. In laboratory measurements τ is typically set between 100–300 µs. Thus, in order to acquire the whole decay process a large number of echos (n_{echo}) is needed. Commonly in laboratory measure-

10 ments several thousand echos are performed within one CPMG sequence. The maximum of all echos detected gives the relaxation curve for estimating the T_2 relaxation time. A classical CPMG sequence is shown in Fig. 2a.

3.2   CPMG with variable τ spacing

For the purpose of using NMR as a borehole tool a significant reduction of energy is

15 needed for conducting a CPMG due to logging requirements for transport and storage of energy.

A reduction of energy is equivalent to a reduction of pulses used (accordingly n_{echo}) for a sequence. As a result of simply reducing the number of echos, the acquisition time is significantly shortened. This leads to errors in the estimated relaxation time, if

20 the decay process is not recorded completely. For compensation the echo spacing τ can be increased. However, a CPMG with an increased constant τ causes insufficient sampling of fast decaying components in the beginning of the decay curve. Thus, it can be expected that a wrong decay time could be estimated. Additionally, diffusion effects will increase too, according to Eq. (3).

25 For that reason we investigated the effect of different variable τ spacings on the estimated decay time. A CPMG sequence with a variable τ is schematically depict in Fig. 2b. The important parameters for constructing a CPMG sequences with a variable τ spacing are the number of echos (n_{echo}) and a minimal and maximal τ. For generating

a sequence with an increasing τ we fixed the values of τ_{min} and τ_{max}. Between these, an amount of n_{echo} linearly increased, exponentially equidistant and logarithmically equidistant τ is calculated. Starting with the lowest possible τ_{min} (τ_1 in Fig. 2b), the fast decaying components are sampled as accurately as possible, while the components with a slow decay are already appropriately sampled.

4   Synthetic study

We conducted a synthetic study to test the evolution of errors for the estimated transverse relaxation time T_2 from CPMG sequences with different ways of increasing τ. First we generated synthetic data of a simple mono-exponential signal to get an overview of the different sequences. Secondly a synthetic multi-exponential signal was generated to evaluate if fast and slow decaying parts within one signal are distinguishable and if both can be determined correctly. Therefore, we used a bi-exponential signal with the transverse relaxation times $T_{2,1}$ and $T_{2,2}$ and fitted the models via a decay time distribution. Finally, to examine influences of diffusion on the data due to an increased τ a diffusive part was added to the synthetic data.

4.1   Mono-exponential signal

A mono-exponential signal can be generated using Eq. (1). The set of model parameter are the initial transverse magnetisation M_0 and the transverse decay time T_2. Here M_0 is set to 1 and the decay time for generating the synthetic data is named T_2^{true} and is varied between 1 ms and 1 s. Standard deviations between the true transverse decay time T_2^{true} (fixed model parameter) and the estimated T_2 of CPMG sequences with a variable τ spacing were calculated for three different noise levels and are plotted in Fig. 3. Each as a function of the true decay time (T_2^{true}) and n_{echo}. All deviations above 20 % are red coloured.

The results for sequences conducted with a small and large constant τ are displayed in the first two rows of Fig. 3. As expected, the error of the estimated decay times increases if n_{echo} is decreasing or the true decay time increases, i.e. slow decaying signals. This is a result of an insufficient acquisition time. If the noise increases, the range of high errors is extended to higher n_{echo} and smaller T_2^{true} (see first row in Fig. 3). Additional errors for small decay times occur if the echo spacing (τ) is increased (second row of Fig. 3), which is probably caused by a bad sampling of fast decaying signals. Thus, increasing a constant τ to compensate the reduction of n_{echo} is not an appropriate approach.

All three sequences with a variable τ spacing, illustrated in the last three rows of Fig. 3, exhibit more or less the same behaviour for the range of errors. Comparing CPMG -sequences with a variable τ spacing with the one using a constant small τ (Fig. 3, first row), smaller errors occur for decreasing n_{echo}, due to the elongated acquisition time. Compared to the sequence with a constant large τ (Fig. 3, second row) all optimized sequences showing smaller errors for fast decaying signals, which is a result of a more tightly sampling of the decay curve at early times. As the noise level is increasing the errors over 20 % expand to sequences with larger n_{echo} and smaller decay times too.

4.2 Bi-exponential signal

In the next step a bi-exponential signal was generated to examine if both, the fast and the slow decaying parts of the signal can be estimated while reducing n_{echo}. For generating the synthetic data Eq. (1) was extended to a sum of two exponentials with the transverse decay times $T_{2,1}$ and $T_{2,2}$. The decay times were chosen in a manner that they are far apart from each other. Therefore, the synthetic decay curve is composed of the decay times $T_{2,1} = 0.01$ s and $T_{2,2} = 1$ s with 5 % noise added. For all sequences with different variable τ spacing the recorded n_{echo} were reduced successively from 1000 to 100 echos.

Title Page

Abstract | Introduction

Conclusions | References

Tables | Figures

|◄ | ►|

◄ | ►

Back | Close

Full Screen / Esc

Printer-friendly Version

Interactive Discussion

The decay curves were fitted with a multi-exponential approach using an inverse Laplace transformation. This calculates corresponding amplitudes to a predefined amount of decay times. For smoothness constraints a Tikhonov regularisation of first kind was used. The regularisation parameter was determined via the L-curve criterion that gives a solution closest to the corner of the L-curve (Aster et al., 2005). The T_2 distributions of the fitted signals are illustrated in Fig. 4 and consists of 100 logarithmically-equidistant-spaced decay times within a range of $T_2 \in [10^{-3}, 10^{1}]$.

In Fig. 4a the signal is sampled with $n_{echo} = 1000$. In all curves a bi-exponential behaviour is observable. Sequences with a small constant τ (blue curve in Fig. 4) can not resolve the slow decaying parts of the signal, due to a short acquisition time (about 0.2 s). As a result the T_2 distribution is broadened and decay times above 3 s are fitted, which exceeds the maximal possible transverse decay time (T_2) of water. Thus, a logarithmic mean decay time of this T_2 distribution will be overestimated.

In contrast, fast decaying components of the signal can not be resolved by a CPMG sequence with a large constant τ spacing (see the black curve in Fig. 4a). This can also be seen in Kleinberg (1994).

Both parts of the signal can be more or less resolved by all sequences with a variable τ spacing. The sequence with an exponentially equidistant τ spacing shows a broadened T_2 distribution for fast decaying components, which is a result of a fast increasing τ that lead to an insufficient sampling of the decay curve for early times.

In general, if n_{echo} is decreasing the bi-exponential behaviour vanishes in conjunction with a broadened T_2 distribution, due to the shortened acquisition time. If n_{echo} is reduced to 200 echos (see Fig. 4c), only sequences with a linearly increased and an exponentially-equidistant τ spacing exhibits a maximum for the slow decaying component. The fast decaying component is resolvable by all sequences. Anyway, the T_2 distribution of $CPMG_{\tau,lin}$ is extended to large decay times.

Title Page

Abstract | Introduction

Conclusions | References

Tables | Figures

◄◄ | ►►

◄ | ►

Back | Close

Full Screen / Esc

Printer-friendly Version

Interactive Discussion

4.3 Bi-exponential signal with diffusion

According to Eq. (4) the τ spacing is the only sequence parameter that influences the diffusion term of an NMR signal. Thus, different ways of increasing τ lead to different impacts of the diffusion on the measured signal. To examine this effect we added a diffusion component to the signal.

According to Coates et al. (1999) the magnetic gradient is influenced by three factors. One depends on the tool design (i.e. tool size, frequency and shape of the used magnet). The second one handles conditions of the formation, such as the temperature. Both are described in chapter 5 in Coates et al. (1999). Here the magnetic gradient of an MRIL tool is denoted with $17\,\mathrm{G\,cm^{-1}}$ while Kenyon (1997) stated that a common magnetic gradient from commercial NMR logging tools is about $20\,\mathrm{G\,cm^{-1}}$. Thereby, we set G to $18\,\mathrm{G\,cm^{-1}}$. Furthermore, the diffusion constant of water $D = 2.5 \times 10^{-9}\,\mathrm{m^2\,s^{-1}}$ was used. The different impacts of G are included by the increased τ. The T_2 distributions for the CPMG sequences with different variable τ spacings and different n_{echo} are plotted in Fig. 5.

Compared to the non diffusive signal (Fig. 4) all T_2 distributions in Fig. 5 are shifted to smaller decay times, except the sequence with constant $\tau = 0.1\,\mathrm{ms}$ (blue curve in Fig. 5). As mentioned before, there are only small influences of diffusion relaxation on the T_2 relaxation time for sequences with a short τ spacing. Nevertheless, the short acquisition time leads to a broadened decay spectrum, which lead to an overestimated log mean decay time. This is more pronounced, if n_{echo} is reduced (see Fig. 5b–d).

Thus, if a variable τ spacing is applied, $T_{2,\mathrm{D}}$ increases for increasing τ_{max} and/or a fast increasing τ. In addition it can be seen that slow decaying components are more influenced by diffusion than the faster ones. This is already visible in Eq. (4). Relative small τ spacings in the beginning of the sequences lead to small influences of diffusion on the signal, but increases successively to larger τ spacing in the end of the sequence.

The largest shifts to short decay times are observable at $\mathrm{CPMG}_{\tau,\mathrm{exp}}$ (see orange curve in Fig. 5), which has the fastest increasing τ spacing. The sequence with a

logarithmically equidistant τ spacing (CPMG$_{\tau,\log}$, red curve in Fig. 5) has the slowest increasing τ and therefore the smallest shift to short decay times. However, it also exhibits the shortest acquisition time and thus lead to the most broadened distribution within the CPMG sequences with a variable τ spacing.

Considering the trade-off between effects due to short acquisition times (broadening) and diffusion (shift to smaller decay times), the CPMG sequence with a linearly increasing τ (Fig. 5, green curve) is superior compared to sequences with an exponentially and logarithmically equidistant τ. Therefore, the CPMG sequence with a linearly increased τ was used for laboratory measurements.

5 Laboratory measurements

As mentioned before, the main effects that influences the estimated T_2 decay time are (i) a shortened acquisition time and (ii) an increased diffusion term, which has to be minimized for the widest possible grain size spectrum. On the other hand the energy consumption for conducting a CPMG sequence has to be minimized, in order to not exceed the possibilities of the borehole tool. The requirement on estimating the T_2 decay time is a minimal or acceptable deviation to a reference sequence. Thus, optimal settings for n_{echo} and $\tau_{\max}$ has to be found. For this purpose laboratory measurements with the Maran Ultra 8 (Resonance Instruments) were conducted.

5.1 Sample preparation and parameter sets of CPMG sequences

Samples of glass beads and granulate with grain size spectra varying from fine silt (fU) to fine gravel (fG) were used. The grain size spectra of the used material are given in Table 1.

For each grain size distribution three samples were prepared. The material was filled in small cylindrical vessels with a hight of $h = 2.6$ cm and a diameter of $d = 3.6$ cm. The sample material was trickled into the vessel, which was filled with distilled water. To

assure comparability of porosity between the three samples of the same material, an ultrasonic bath was used to raise the packing density to a maximum. Afterwards the samples were filled up and sealed with a foil to minimize evaporation effects during NMR measurements. To avoid further heating during NMR measurements and thus
5 temperature effects on the initial amplitude and the decay time (Godefroy et al., 2001) the samples were heat up to 25–30 °C. The samples were weighted before and after NMR measurements to appraise a possible evaporation during the NMR measurements. Variations of the mass less than 1 % were observed.

If a sample is completely water saturated the porosity can be calculated using the
10 initial amplitude. A comparison between the NMR- and gravimetric-porosity is illustrated in Fig. 6, which is an easy way to determine if any faults were made during the preparation or measurement.

We performed 9 CPMG sequences per sample with different values of τ_{max} and n_{echo}. The logarithmic mean of the T_2 distribution were compared with the log mean decay
15 time ($T_{2,lg}$) of the reference sequence, which consists of 5000 pulses and a constant τ of 300 µs. The pulse-echo spacing is increased in a linear manner staring with $\tau_{min} = 100$ µs while τ_{max} was set between 400 and 4000 µs. The minimal echo spacing (τ_{min}) was the lowest possible value that could be realized with the Maran Ultra 8. The amount of echos was decreased beginning with $n_{echo} = 500$ down to $n_{echo} = 50$. By choosing
20 these sequence parameters an outline of the effect on the acquisition time together with diffusion effects for different grain sizes, i.e. signals with different decay times, can be obtained. A full list of the main sequence parameters n_{echo} and τ_{max} together with the resulting acquisition time t_{tot} is given in Table 2.

5.2 Results

5.2.1 T_2 distribution of glass beads

25 The T_2 distribution of different glass beads are illustrated in Fig. 7. The mean grain size spectra is increasing from top to bottom, in which samples of coarse silt (40–70 µm) are

depict in the first row (Fig. 7a–c), samples of medium sand (250–500 µm) in the second row (Fig. 7d–f) and samples of coarse sand (1250–1650 µm) in the third row. The echos are decreasing form left to right starting with $n_{echo} = 500$ down to $n_{echo} = 50$. Within each subplot of Fig. 7 the blue coloured T_2 distribution is associated with the reference sequence. The other curves denotes CPMG sequences with a linearly increasing τ spacing and different τ_{max} values. The corresponding log mean decay times of the distribution are given in Table 3.

For $n_{echo} = 500$ (Fig. 7a) the T_2 distribution for fine-grained glass beads are displayed. Compared to the reference sequence a shift of the main peaks to smaller decay times is observed, which is more distinctive for an increasing τ_{max}. For a constant n_{echo} the τ spacing increases faster for larger τ_{max}. Thus, considering Eq. (3) a larger τ lead to a higher attenuation due to diffusion and results in a larger shift to smaller decay times.

For $n_{echo} = 500$ and increasing the grain size (from top to bottom) it shows that a shift to small decay times is observed for all grain sizes. For the fine-grained sample (Fig. 7a) the difference of the main peak to the reference signal is about 55.65 ms considering the sequence with $\tau_{max} = 4000$ ms, while the shift for the medium-grained sample (Fig. 7d) is, with a difference of 164 ms, increased. Beside this, for coarse sand samples the shift decreases with a larger τ_{max}, which is due to the short acquisition time. For coarse-grained material NMR signals decay more slowly, due to an decrease of $\frac{S}{V}$ of the surface relaxation $T_{2,S}$. Thus, maintaining the sequence parameter (n_{echo}, τ_{max}) the acquisition time is getting insufficiently short for slow decaying signals and small τ_{max}. Furthermore, the shorter acquisition time leads to a broadening of the T_2 distribution.

For decreasing n_{echo} (from left to right) and fine-grained material the same effect of broadening is observed, however in addition to fully acquiring the signal, the sampling of the decay curve is the key factor. If the decay is completely acquired by the CPMG sequence, as it is the case for the fine-grained material and sequences with $\tau_{max} = 4000$ µs, the reduction of data points due to decreased n_{echo} leads to a broadening of the T_2

distributions. If the signal is not completely acquired as it is the case for $\tau_{max} = 400$ µs a further broadening is observed.

For decreasing n_{echo} and increasing the grain size it shows that the effect of acquiring the complete signal is dominating the data sampling effect. Theoretically a shortened acquisition time due to a reduction of n_{echo} can be compensated by a larger τ_{max}, however this leads to higher diffusion.

5.2.2 Log mean decay time of glass beads

The corresponding log mean decay times ($T_{2,lg}$) to the T_2 distributions of glass beads are given in Table 3. For each sample and amount of echos (n_{echo}) a systematic decrease of $T_{2,lg}$ for an increasing τ_{max} is observable. On the one hand this can be explained by an attenuated diffusion for fast decaying signals, which are fully acquired. On the other hand for slower decaying signals the decrease of $T_{2,lg}$ results from the broadening of the T_2 distribution due to an insufficient acquisition time.

If n_{echo} is reduced $T_{2,lg}$ is decreasing for silt and medium sand samples with $\tau_{max} = 1000$ and 4000 µs, which is also an effect of acquisition time. In contrast, the sequence with $\tau_{max} = 400$ µs of medium sand and all sequences of coarse sand samples showing an increasing $T_{2,lg}$ if n_{echo} is decreasing. This is a result of a flattened T_2 distribution with large decay times (beyond 3 s) fitted to explain the data.

Sequences conducted for example with $n_{echo} = 500$ and $\tau_{max} = 400$ µs seems to overestimate $T_{2,lg}$ compared to the reference sequence (silt and medium-grained glass beads in Table 3), although the decay process is recorded completely. Compared to the reference sequence, fast decaying components are vanished in the T_2 distributions (see Fig. 7). A cut off time for calculating $T_{2,lg}$ could possibly solve that problem.

5.2.3 T_2 distribution of granulate samples

The T_2 distributions for granulate samples are illustrated in Fig. 8. Sequences with $n_{echo} = 50$ are neglected, because the T_2 distribution of glass beads (see Fig. 7c, f,

i) showed that the acquisition time is to short for getting appropriate results. Also the results for fine gravel are neglected, because these large grained materials are assumed to have already good hydraulic properties, whose estimation was one of the major focuses.

In comparison to the glass beads, the T_2 distribution of granulate exhibits a bi-exponential behaviour which is more distinctive at coarse sand (Fig. 8c and d). Consistent with the glass beads the shift of the T_2 distribution to smaller decay times is observable too. In contrast to the fine material of glass beads (see Fig. 7a) the shift is getting more distinctive for decreasing τ_{max}. It can be assumed that a insufficient acquisition time caused this effect, since an increased diffusion term leads to an increasing shift for larger τ_{max}.

The absolute shift also increases with grain size, which could be an interaction of attenuated diffusion for increasing grain size and a short acquisition time. According to Fig. 8a and c, a flattening of the T_2 distribution for coarse-grained material is observable too.

A reduction of n_{echo} is shortening the record time to and thus leads to broadened T_2 distribution. Additionally, as a result the bi-exponential behaviour is vanishing.

5.2.4 Log mean decay time of granulate samples

In agreement with the results of glass beads, $T_{2,lg}$ of the granulate (see Table 4) is decreasing if τ_{max} increases and is explainable in the same way. Due to an insufficient acquisition time $T_{2,lg}$ increases for sequences with $\tau_{max} = 400$ and $1000\,\mu s$ of coarse sand and CPMG sequence with $\tau_{max} = 400\,\mu s$ of medium sand.

Apparently, $T_{2,lg}$ of the medium-grained granulate (first row in Table 4) is quite similar to the log mean decay time of fine-grained glass beads (Table 3, first row). Knowing that a different surface to volume ratio (S/V) of these two samples can be assumed (according to different mean grain size spectra), a change in the surface relaxivity (ρ) and/or changing internal magnetic gradients (G) is a way to compensate this, in order to get comparable decay times.

6 Conclusions

As part of a project for developing an NMR borehole tool to characterise near surface groundwater layer in unconsolidated material optimized CPMG sequences for measuring T_2 decay time were examined.

A synthetic study of sequences with an exponentially-, logarithmically-equidistant nd linearly increased echo spacing showed that decay times of mono- and multi-exponential signals can be resolved with respect to the sequence parameters. It can also be seen that the sequence with a linearly increasing τ yields the best results for slow and fast decaying components if diffusion is taken into account.

Laboratory measurements on glass beads and granulate of different grain size spectra showed that the main sequence parameters (n_{echo} and τ_{max}) cannot be chosen arbitrarily. Regarding the usage of NMR data, for example to estimate the hydraulic conductivity, a sequence with 500–200 echos and $1000\,\mu s \geq \tau_{max} \leq 2500\,\mu s$ is an appropriate choice. Because coarse-grained material is of minor interest, due to the high hydraulic conductivity, slow decaying signals do not have to be fitted too. Although, by adapting the sequence parameters it is possible to fit NMR data of coarse material with an acceptable accuracy. Therefore, an application of a CPMG sequence with a variable echo spacing to obtain slow and fast decaying components instead using two CPMG sequences seems to be feasible, which results in faster measurements and thus an increased vertical resolution. A field test within an calibration pit is demanded to show the applicability under borehole conditions. Further investigation is needed to examine the behaviour on natural material. A closer look on the influence of different magnetic gradients on CPMG sequences with an increasing τ is of high interest.

Back | Close

Full Screen / Esc

Printer-friendly Version

Interactive Discussion

References

Aster, R., Borchers, B., and Thurber, C.: Parameter Estimation and Inverse Problems, Elsevier Academic Press, 2005. 517

Bloch, F., Hansen, W. W., and Packard, M.: The Nuclear Induction Experiment, Phys. Rev., 70, 474–485, doi:10.1103/PhysRev.70.474, 1946. 509

Brown, R. and Gamson, B.: Nuclear, magnetism logging, J. Petrol. Technol., 12, 199–207, 1960. 509

Brownstein, K. R. and Tarr, C. E.: Importance of classical diffusion in NMR studies of water in biological cells, Phys. Rev. A, 19, 2446–2453, doi:10.1103/PhysRevA.19.2446, 1979. 513

Carr, H. Y. and Purcell, E. M.: Effects of Diffusion on Free Precession in Nuclear Magnetic Resonance Experiments, Phys. Rev., 94, 630–638, doi:10.1103/PhysRev.94.630, 1954. 509, 512

Coates, G., Xiao, L., and Prammer, M.: NMR Logging Principles and Application, Halliburton Energy Services, 1999. 511, 518

Dunn, K. J., Bergman, D. J., and Latorraca, G. A.: Nuclear magnetic resonance, 1st Edn., Pergamon, 2002. 511

Godefroy, S., Fleury, M., Deflandre, F., and Korb, J.-P.: Temperature effect on NMR surface relaxation, in: SPE Annual Technical Conference and Exhibition, 30 September–3 October 2001, New Orleans, Louisiana, doi:10.2118/71700-MS, 2001. 520

Hahn, E. L.: Spin Echoes, Phys. Rev., 80, 580–594, doi:10.1103/PhysRev.80.580, 1950. 509

Keating, K. and Knight, R.: A laboratory study to determine the effect of iron oxides on proton NMR measurements, Geophysics, 72, E27–E32, doi:10.1190/1.2399445, 2007. 512

Kenyon, W. E.: Petrophysical Principles of Applications of NMR Logging, The Log Analyst, 38, 21–43, 1997. 518

Kleinberg, R.: Pore size distributions, pore coupling, and transverse relaxation spectra of porous rocks, Proceedings of the Second International Meeting on Recent Advances in MR Applications to Porous Media, Magnetic Resonance Imaging, 12, 271–274, doi:10.1016/0730-725X(94)91534-2, 1994. 517

Kruspe, T., Thern, H. F., Kurz, G., Blanz, M., Akkurt, R., Ruwaili, S., Seifert, D., and Marsala, A. F.: Slimhole Application of Magnetic Resonance While Drilling, in: Proceedings of SPWLA 50th Annual Logging Symposium, Society of Petrophysicists and Well-Log Analysts, 2009. 509

Title Page

Abstract | Introduction

Conclusions | References

Tables | Figures

◄◄ | ►►

◄ | ►

Back | Close

Full Screen / Esc

Printer-friendly Version

Interactive Discussion

Meiboom, S. and Gill, D.: Modified Spin-Echo Method for Measuring Nuclear Relaxation Times, Rev. Sci. Instrum., 29, 688–691, doi:10.1063/1.1716296, 1958. 509, 512

Miller, M., Paltiel, Z., Gillen, M., Granot, J., and Bouton, J.: Spin Echo Magnetic Resonance Logging: Porosity and Free Fluid Index Determination, in: Proceedings of SPE Annual Technical Conference and Exhibition, Society of Petroleum Engineers, doi:10.2118/20561-MS, 1990. 509

Purcell, E. M., Torrey, H. C., and Pound, R. V.: Resonance Absorption by Nuclear Magnetic Moments in a Solid, Phys. Rev., 69, 37–38, doi:10.1103/PhysRev.69.37, 1946. 509

Seevers, D. O.: A nuclear magnetic method for determining the permeability of sandstones, in: Proceedings of SPWLA 7th Annual Logging Sympsdium, Society of Petrophysicists and Well-Log Analysts, 1966. 509

Optimization of CPMG sequences for NMR borehole

M. Ronczka and
M. Müller-Petke

Title Page

Abstract | Introduction

Conclusions | References

Tables | Figures

◄◄ | ►►

◄ | ►

Back | Close

Full Screen / Esc

Printer-friendly Version

Interactive Discussion

Table 1. Grain size spectra of different samples for glass beads and granulate used in laboratory measurements, with fU, mU: fine, medium silt; fS, mS, gS: fine, medium, coarse sand; fG: fine gravel.

	glass beads d [µm]	granulate d [µm]
fU – mU	0–50	–
gU	40–70	–
fS	90–150	–
mS	250–500	250–500
gS	1250–1650	1000–1600
fG	3800–4400	3000–6000

Table 2. Sequence parameter for the tested CPMG sequences. Starting from a fixed $\tau_{min} = 100\,\mu s$ the echo spacing was increased up to τ_{max}, which equals to the total acquisition time t_{tot} given in column 3.

n_{echo}	τ_{max} [ms]	t_{tot} [s]
500	4000	2.05
	1000	0.55
	400	0.25
200	4000	0.82
	1000	0.22
	400	0.1
50	4000	0.205
	1000	0.055
	400	0.025

Optimization of CPMG sequences for NMR borehole

M. Ronczka and
M. Müller-Petke

Table 3. Logarithmic mean decay time $T_{2,lg}$ for all CPMG sequences conducted on glass beads. The second column denotes $T_{2,lg}$ of the reference sequence conducted with $n_{echo} = 5000$ and a constant $\tau = 300\,\mu s$.

sample	$T_{2,lg}$ [ms] (reference)	τ_{max} [μs]	n_{echo}: 500 ($T_{2,lg}$ [ms])	200 ($T_{2,lg}$ [ms])	50 ($T_{2,lg}$ [ms])
silt		400	91.55	81.78	75.02
(40–70 μm)	73.25	1000	76.91	68.22	53.40
		4000	59.38	46.7	30.85
medium-grained		400	592.58	761.54	1083.6
(250–500 μm)	487.68	1000	508.07	461.41	454.01
		4000	457.52	424.97	378.58
coarse-grained		400	1721.7	1869.1	1824.6
(1250–1650 μm)	1320.1	1000	1543.1	1728.4	2057.6
		4000	1366.6	1589.1	1405.8

Table 4. Logarithmic mean decay time $T_{2,\lg}$ for all CPMG sequences conducted on granulate samples. The second column denotes $T_{2,\lg}$ of the reference sequence conducted with $n_{echo} = 5000$ and a constant $\tau = 300\,\mu s$.

sample	$T_{2,\lg}$ [ms] (reference)	τ_{max} [µs]	n_{echo}: 500 ($T_{2,\lg}$ [ms])	200 ($T_{2,\lg}$ [ms])
mS (250–500 µm)	89.04	400	100.22	102.91
		1000	93.9	88.46
		4000	84.75	77.25
gS (1000–1600 µm)	264.15	400	326.84	343.51
		1000	268.97	346.18
		4000	262.47	264.3
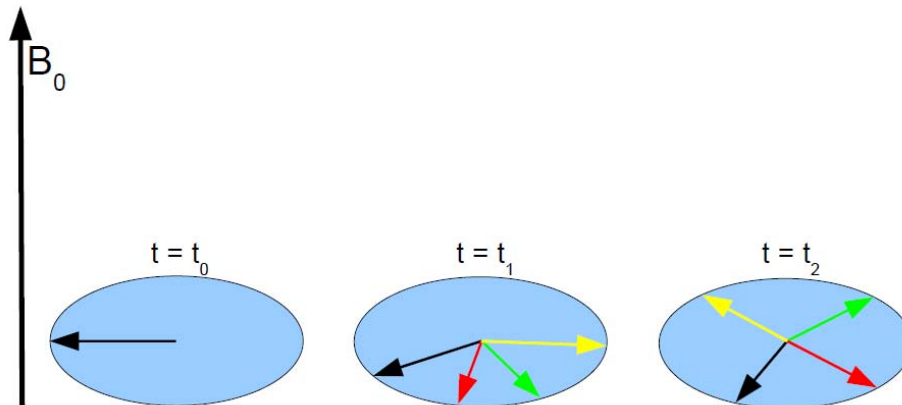
Fig. 1. Loss of phase coherence of protons due to differences in the Larmor frequency in the presence of magnetic gradients.
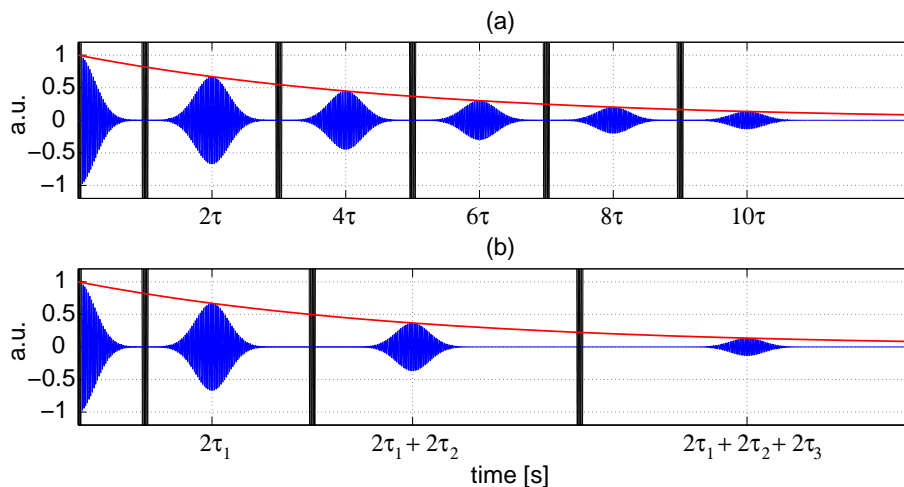
Fig. 2. (a) Classical CPMG sequence with a P90 excitation pulse and several P180 pulses for refocusing. After each P180 pulse an echos appears. The envelope of all detected echos gives the T_2 decay curve. **(b)** First pulses and the resulting echos for a CPMG sequence with variable τ spacing.
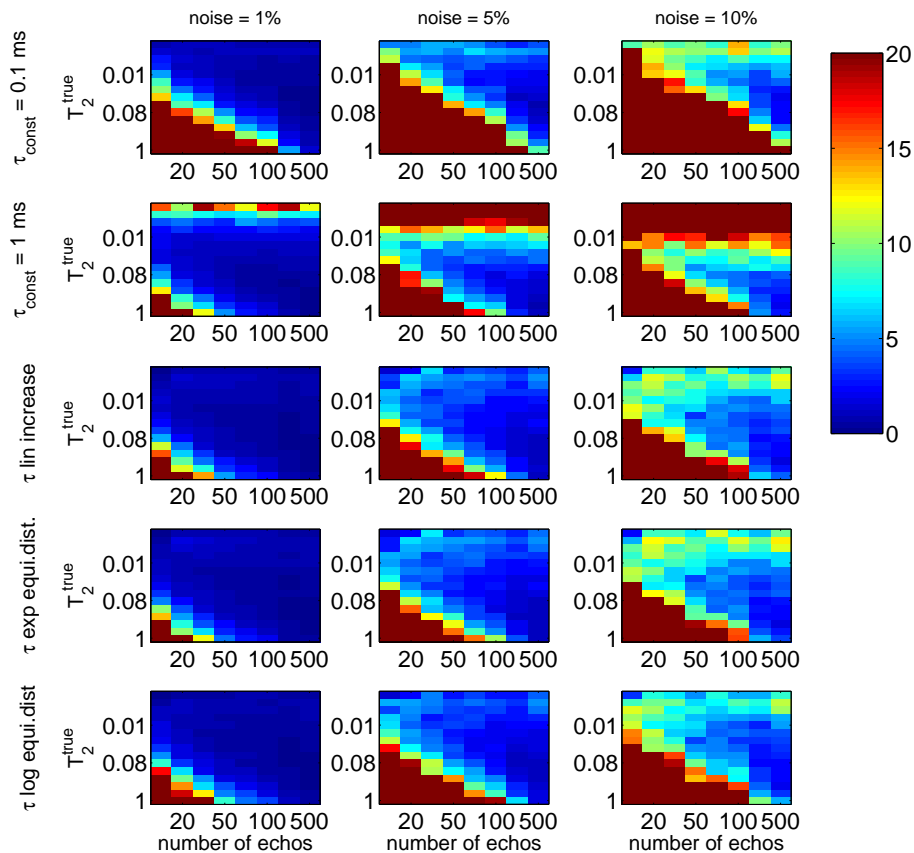
Fig. 3. The evolution of error for different signal-to-noise ratio. Standard deviations between the true transverse decay time T_2^{true} and the estimated T_2 depending on the number of echos for mono-exponential synthetic data is shown. All errors over 20 % are red coloured.

Title Page

Abstract | Introduction

Conclusions | References

Tables | Figures

◄ | ►

◄ | ►

Back | Close

Full Screen / Esc

Printer-friendly Version

Interactive Discussion
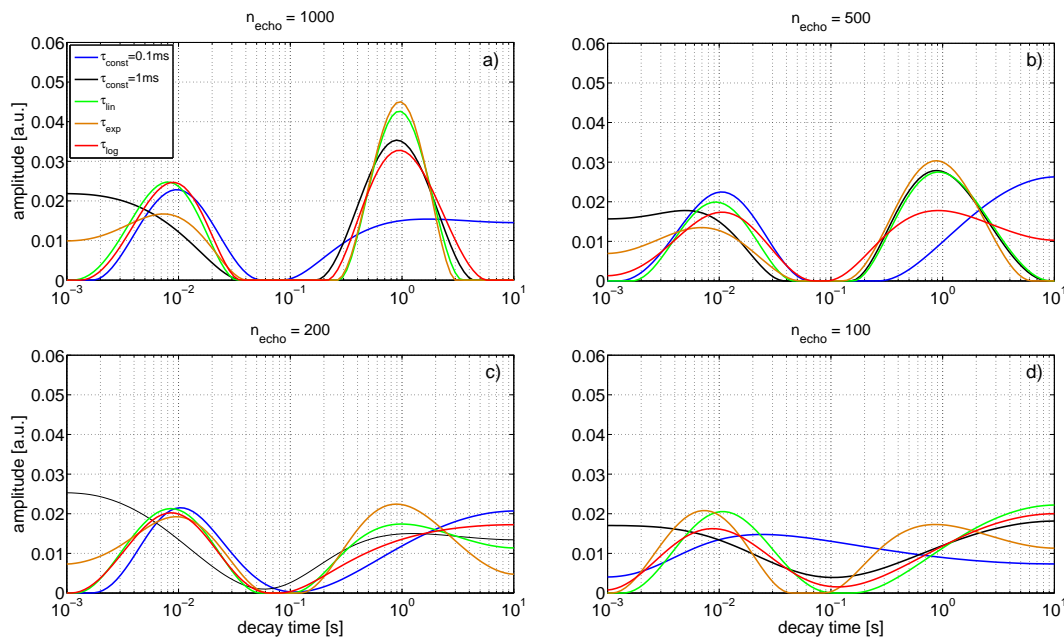
Fig. 4. T_2 distributions of bi-exponential signals with different n_{echo} beginning with 1000 echos **(a)** to 100 echos **(d)** all with 5 % noise added. Sequences with linearly increasing, exponentially equidistant and logarithmically equidistant τ spacing with $\tau_{max} = 2$ ms are plotted. Additionally two sequences with an constant τ spacing are shown.
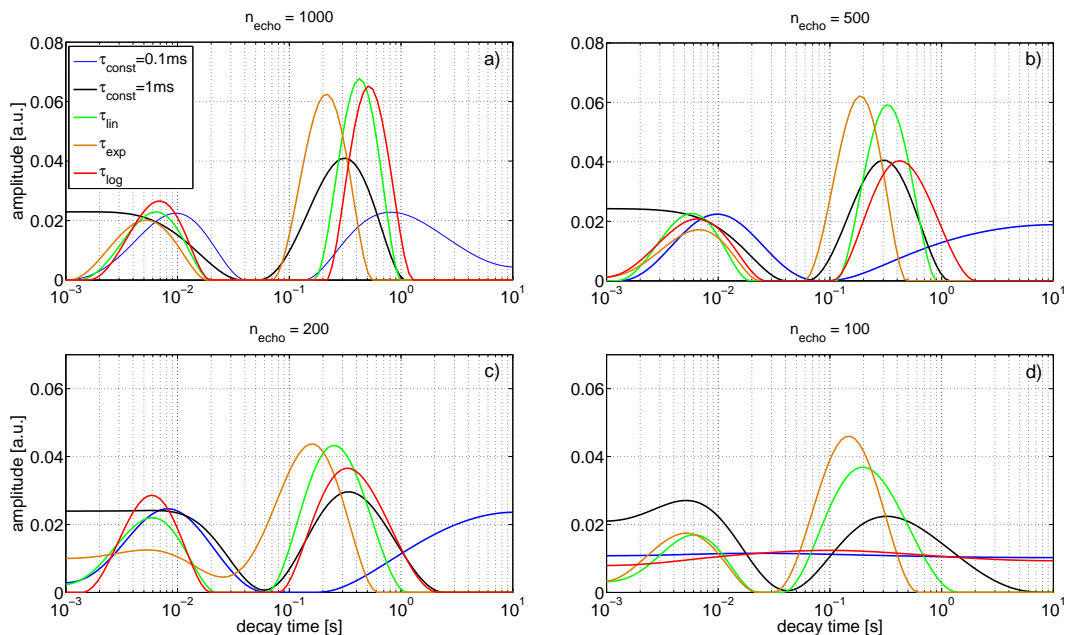
Fig. 5. T_2 distribution of a bi-exponential signal with $T_{2,1} = 0.01$ s and $T_{2,2} = 1$ s with a diffusion component added and 5 % noise. CPMGs with linearly increasing, exponentially equidistant and logarithmically equidistant τ spacing with $\tau_{max} = 2$ ms are plotted for different amounts of echos. Additionally two sequences with an constant τ spacing are plotted.
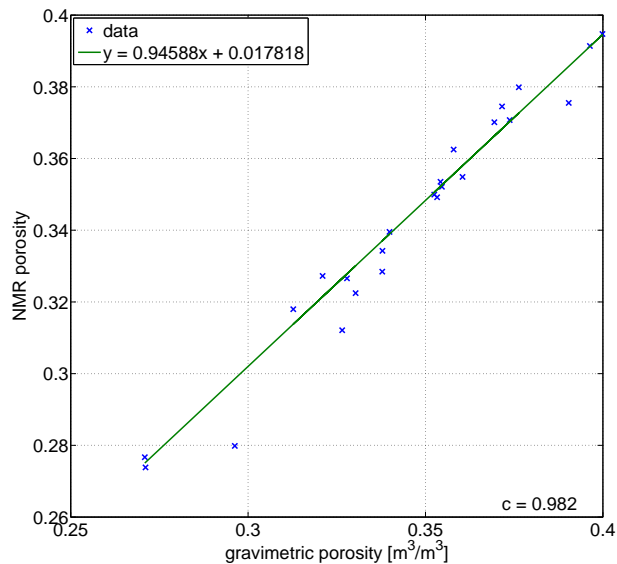
Fig. 6. Cross-plot of porosities determined via NMR- and gravimetric-measurements. The NMR-porosity is in excellent agreement with the gravimetric ones, which is validated by the correlation coefficient of $c = 0.982$.

Optimization of CPMG sequences for NMR borehole

M. Ronczka and
M. Müller-Petke

Title Page

Abstract | Introduction

Conclusions | References

Tables | Figures

◄◄ | ►►

◄ | ►

Back | Close

Full Screen / Esc

Printer-friendly Version

Interactive Discussion
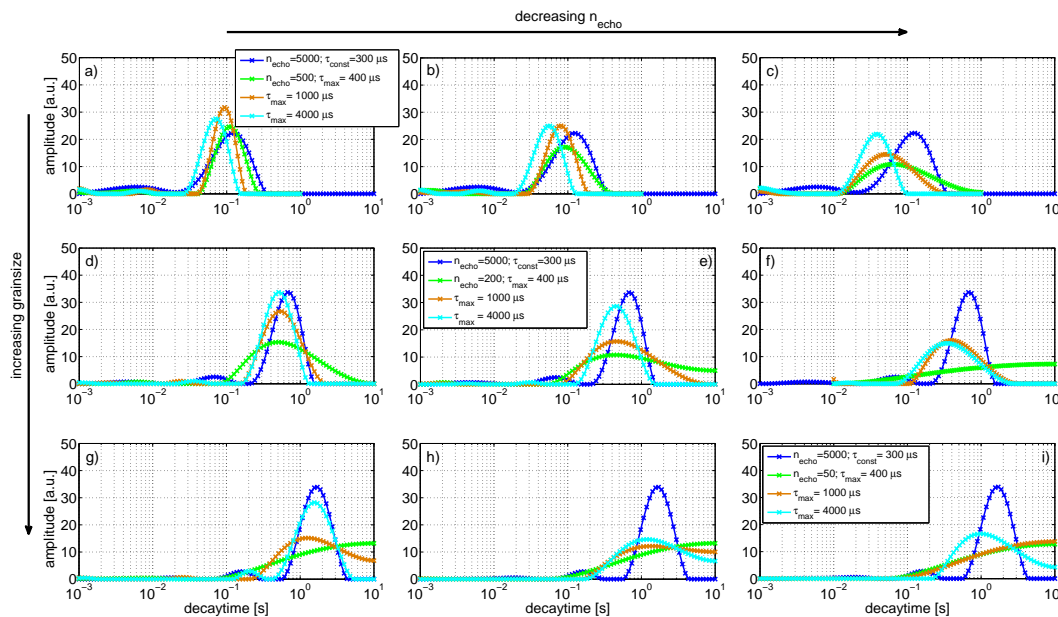
Fig. 7. T_2 distribution of glass beads for CPMG sequences with a linearly increased τ. Columns indicates a decreasing n_{echo} (500–200–50, also given in the legends). The grain size increases from top to bottom (first row – coarse silt; second row – fine sand; third row – coarse sand).
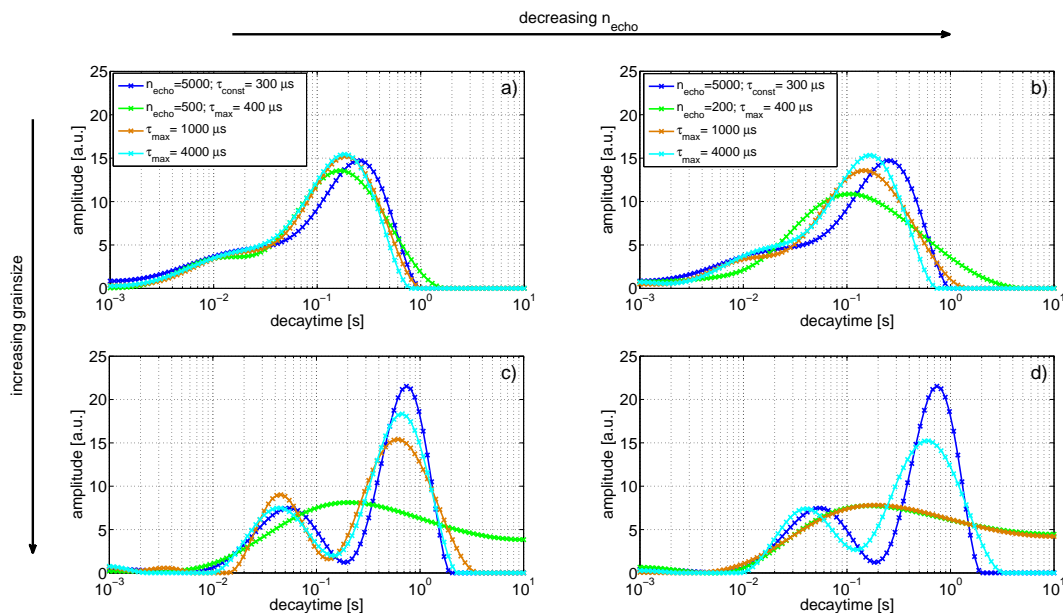
Fig. 8. T_2 distribution of granulate for pulse sequences with a linearly increased τ. n_{echo} is decreasing from left to right beginning ($n_{echo} = 500$–200). The grain size increases from top (medium sand) to bottom (coarse sand).